Article:

Shirley, R, Hawthorne, J and Black, L (2015) Waste incinerator residue treatment: Variability implications. Proceedings of the Institution of Civil Engineers: Waste and Resource Management. ISSN 1747-6526

https://doi.org/10.1680/warm.14.00002

Waste Incinerator Residue Treatment: Variability Implications

Robin Shirley*PhD, MSc, BSc, **Josh Hawthorne** **MSc, MEng**, **Leon Black** PhD, MSc, BSc,

Institute for Resilient Infrastructure, School of Civil Engineering, University of Leeds, Leeds, LS2 9JT, UK

*Corresponding Author, r.a.shirley@leeds.ac.uk, +44 113 343 2248

Word Count: 4993

Number of Figures: 7

Abstract

Air pollution control residues are a hazardous waste, collected when controlling the flue gas emissions created within modern energy from waste incinerators. They are inherently variable with regards to mineralogy and morphology. However, this variability is frequently neglected throughout the scientific literature concerned with their management. This work characterises residues collected from five different UK facilities and highlights the implications of their compositional variability for the performance of products resulting from a stabilisation/solidification treatment. It is demonstrated that the variability is of significance for the mineralogy and several key engineering properties of the products, and links between the properties of the residues and the behaviour of the products are shown. Residue variability should be considered when researching technical management options. Treatments are likely to require modification in order to satisfy performance envelopes for individual batches of residue.

Keywords

Waste Management and Disposal

Materials Technology

Research and Development

1 Introduction

Air pollution control (APC) residues are collected in order to comply with regulatory air emissions limits associated with solid waste incineration in modern energy from waste (EfW) facilities (EC 2010). Residues collected from dry or semi-dry scrubber systems generally consist of particulate matter carried in the gas stream (i.e. the ‘fly ash’), together with surplus reactants and products resulting from the injection of an alkaline scrubber used to neutralise acid gases. Activated carbon is also injected into the gas stream to adsorb organic pollutants and highly volatile metals which may be present in the vapour phase (International Ash Working Group 1997; Williams 2005). A reactant such as urea or ammonia may also be used to convert NOx gases to nitrogen and water (Williams 2005).

The resultant residues have an absolute entry in the European Waste Catalogue (EWC 19 01 07*) and typically show hazardous properties defined in Annex III of the Waste Framework Directive (EC 2008) including H4 (irritant) due to the alkalinity, and H14 (ecotoxic) due to the heavy and toxic metals contained. A major concern when considering disposal of the residues is the very high concentration of soluble chloride and sulphate salts which result from acid gas neutralisation (Bodenan and Deniard 2003). Inappropriate disposal of the residues can result in salination of groundwater, degrading an important natural resource (EC 2006).

As stated by the International Ash Working Group (International Ash Working Group 1997) “Beginning with the type of waste feed to the incinerator, everything which occurs prior to, and during, the collection of the APC residues, may affect the characteristics and quantities of the captured residues.” Of particular importance is the design and operation of the APC system. The various systems available for the control of air pollution from such facilities have been comprehensively reviewed in textbooks including (International Ash Working Group 1997; Williams 2005). The current work is concerned with residues resulting from typical dry or semi-dry scrubber systems which include the fly ash. Unless otherwise stated such residues will be referred to as APC residues within this article. Lime scrubbers are most commonly used in such systems, which results in residues containing high levels of calcium salts. However, sodium based scrubbers are also used occasionally (Geysen et al. 2004a; Jacquinot et al. 2000). Variability in the concentration of minor and trace elements, chloride and sulphate salts, and the quantity of residual scrubber present can also be seen throughout the literature concerned with APC residue composition and treatment methods e.g.(Baciocchi et al. 2009; Cappai et al. 2012; De Boom and Degrez 2012; Dyer et al. 2006; Geysen et al. 2004b; Li et al. 2007; Quina et al. 2008b; Wang et al. 2010). Residue properties vary not only between facilities but also over time when collected from a single facility (Environment Agency 2002; Quina et al. 2008b).

Options for minimising the environmental impact of APC residues have been extensively researched and reviewed (Amutha Rani et al. 2008; Quina et al. 2008a). One option which has received considerable attention is treatment by stabilisation/solidification (s/s)(Alba et al. 2001; Dyer et al. 2006; Geysen et al. 2004b; Kougemitrou et al. 2011; Lampris et al. 2011; Shirley and Black 2011b). The high level of variability in the mineralogy and morphology of APC residues may have significant implications for the behaviour and properties of s/s products because the properties of freshly blended cements, the process of cement hydration, and the resultant microstructure of cementitious matrices are all sensitive to the chemistry and physical properties of the system (Neville and Brooks 1994; Taylor 1997). Residue variability may therefore necessitate modification of treatment processes in order to satisfy legal and recommended (Stegemann and Zhou 2009) performance envelopes. The aim of the current study was to investigate the implications of waste variability when using s/s as a treatment option for APC residues. This was accomplished by characterising residues resulting from five different EfW facilities throughout the UK, and applying the same s/s treatment to each of the residues. The performance and characteristics of the resultant products were discussed in terms of the initial residue composition, and the criteria considered critical to the success of the treatment option (Stegemann and Zhou 2009) and required by European waste acceptance criteria (WAC) (EC 2003).

2 Materials and Methods

2.1 Materials

APC residues were collected from five different UK EfW incinerators, all of which operate as mass burn facilities and use a semi-dry, $Ca(OH)_2$ based scrubber process which also involves the injection of activated carbon. Residues were collected from the fabric filters and incorporate the fly ash. The nomenclature A1-A5 was used to identify the residues. Residue A1 was obtained from a facility in which clinical waste is incinerated whilst residues A2-A5 were all obtained from facilities in which residual municipal solid waste (MSW) was incinerated. S/S treatment was applied using a CEM I 52.5N (Castle cement) as the binder. A waste:binder ratio of 2:3 by weight was employed and a liquid to solid ratio (l/s) by weight of 0.5 using 18 MΩ de-ionised water as the liquid phase. Blends were mixed by hand until a homogeneous paste was achieved and cast as 50mm cubes which were filled in two layers and compact using a vibrating table. Samples were cured at room temperature, in sealed plastic bags to prevent drying and excessive carbonation, until test age. The s/s samples were designated the nomenclature 2:3 AX (in which X ranges from 1 to 5), identifying the waste:binder ratio and the residue incorporated.

2.2 Mineralogical and Morphological Characterisation Techniques

Simultaneous thermogravimetric and differential thermal analysis was performed using a Stanton-Redcroft STA1500. Single samples weighing 10-18 mg were heated in a platinum crucible and flowing N_2 atmosphere, from 20-900°C at a heating rate of 20°C/min. Compounds were identified based on decomposition temperatures previously determined and reported throughout the literature. Quantification was achieved by drawing tangents to the thermogravimetric analysis (TGA) curve and measuring the weight loss at the midpoint, before calculating the compound concentration based on molecular weights and decomposition reactions (Shirley and Black 2011b). The as-received (untreated) residues underwent overlapping mass losses due to the dehydroxylation of $Ca(OH)_2$ and CaClOH, preventing resolution of the loss by each compound. In order to approximate the quantities of each compound in the residues, the area of the endothermic $Ca(OH)_2$ peak recorded by differential thermal analysis (DTA) was compared with a linear calibration curve (DTA peak area per mg of sample against %w/w determined by TGA), establishing the %w/w $Ca(OH)_2$. The mass loss attributable to this concentration was then subtracted from that observed in the region of the overlapping losses and the remainder attributed to dehydroxylation of CaClOH. Finally concentrations were converted to a percentage of the dry weight of the residue in the as-received condition. Calibration curves and further discussion of the method are shown in Appendix A.

XRD analysis was performed using a Phillips X'pert Pro diffractometer with X'celerator detector; Cu Kα x-ray source operated at 40kV and 40mA; Ni β filter; 0.04 radian Soller slits; and divergence and anti-scatter slits programmed to give an irradiated/observed length of 10mm. Data was typically collected with a step size of 0.0334°2θ and a time per step of 120 seconds. Samples were analysed between 5-60°2θ.

Morphology was examined by specific surface area measurements. Gas sorption isotherms for the APC residues were collected with N_2 at 77K using a Micromeritics TriStar 3000. Samples were outgassed at 80°C under a flowing N_2 atmosphere until a constant weight (deviation <0.1% of initial mass over a four hour period) was achieved. Surface area was determined using the BET equation assuming a N_2 molecular cross sectional area of $0.162nm^2$. BET plots showed coefficients of determination>0.999 and were established using five data points between relative pressures of 0.05-0.25. Due to the high C values observed for some samples, an assessment of microporosity was made using the t-plot method (Sing 1982). Isotherms were compared against the universal t-curve fitted with the isotherm equation of Harkins and Jura, as established by de Boer et al (de Boer et al. 1966).

2.3 Performance Testing

Workability was measured by flow table (BS EN 1015-3:1999), setting time by Vicat needle penetration (BS EN 196-3:2005) and compressive strength using 50mm cubes according to the method described in (BS EN 12390-3:2009). Compressive strength was also determined, after 7 days submersion in de-ionised water, following the procedure described by Stegemann and Zhou (Stegemann and Zhou 2009), and after completion of the monolithic leach test EA NEN 7375:2004. Bulk porosity was determined according to the equation presented by Lampris et al (Lampris et al. 2009). True density of the residues and products was determined using a Quantachrome Ultrapycnometer 1000 with helium gas. As-received residues were prepared for pycnometry by drying at 60°C and blends were dried by immersion in isopropanol for 24 hours followed by vacuum drying.

Leaching tests were performed using the standard methods required to evaluate against UK waste acceptance criteria (UK Statutory Instruments 2005; UK Statutory Instruments 2010). Granular leach testing was performed according to BS EN 12457-2:2002 adapted to use 10g (dry mass) samples and a rotating table operated at 90rpm. Monolithic leach testing was performed according to EA NEN 7375:2004 using 50mm cubes. 18 MΩ de-ionised water was used for all leach and acid neutralisation capacity testing. The pH of leachates from both test procedures was determined using a pH meter calibrated with buffer solutions of pH=4, 7 and 9.2. Total dissolved solids (TDS) in the granular leachates was determined according to BS EN 15216:2007. Leachates were stored in accordance with BS EN ISO 5667-3:2003 and analysed for anions using a Dionex DX500 liquid chromatograph system with IonPac AS14 anion exchange column and ED40 electrochemical detector.

Acid neutralisation capacity (ANC) of the as-received residues and s/s products was tested by establishing an initial liquid to solids ratio of 9 using 5g (dry mass) of sample. Samples were continuously agitated using a rotating table and titrated by addition of 0.5 or 1mEq/g using a 70% HNO_3 solution in order to minimise changes to the liquid to solids ratio. pH was measured after allowing solids to settle and considered stable once a deviation of <0.3 pH units was observed over a 24 hour period. This test method is similar to that described by Young et al (Young et al. 1988) and Annex B of DD CEN/TS 15364:2006, with modified sample size and equilibration times.

Isothermal conduction calorimetry was performed using an 8 channel TAM Air calorimeter operated at 20°C. Total sample mass was 8g. Samples were mixed mechanically for 60 seconds before loading into the calorimeter. Reference ampoules contained 6g of quartz sand and 3g of water.

3 Results and Discussion

3.1 Characterisation of as-received residues

Table 1 Analysis of as-received residues including pH and release of Cl, SO_4 and TDS during BS EN 12457-2, alkalinity to pH 4.5 presented as %$CaCO_3$ equivalent, concentration of compounds evident from STA (%w/w_{dry}), density and specific surface area determined by N_2 sorption isotherms.

N_2 sorption isotherms for all residues were type IIb according to classifications described by Rouquérol et al (Rouquérol et al. 1999) (Appendix B). This type of isotherm is commonly associated with aggregated powders. BET surface areas are presented in Table 1. Values can be seen to differ by as much as 19.9m^2/g. Quina et al reported BET surface areas between 4.9-6.8m^2/g for five separate collections of semi-dry APC residues, from a Portuguese EfW incinerator over a two year period (Quina et al. 2008b). The variability in the specific surface area of residue collected from a single facility over time was therefore much smaller than that observed for residues collected from different sites.

True densities of the residues were all between 1900 and 2600kg/m^3 (Table 1) and generally showed sensible agreement with the density of the principal compounds present (e.g. density (kg/m^3) of $Ca(OH)_2$=2343; $CaCO_3$=2711; $CaSO_4$=2960; NaCl=2170; KCl= 1988 (Dean and Lange 1999)). Residue A3 for example, was observed by thermal analysis and XRD to contain large amounts of calcite which was reflected in the true density. Quina et al (Quina et al. 2008b) observed a consistent and similar true density of 2500-2600kg/m^3.

The mineralogy of the residues was similar to that observed for semi-dry scrubber residues previously studied (Bodenan and Deniard 2003; Cappai et al. 2012; Lampris et al. 2009). XRD patterns for the as-received residues together with those for the matched crystalline phases are presented in Figure 1. Quantification of the phases which were also identifiable by thermal analysis ($Ca(OH)_2$, $CaCO_3$ and CaClOH) are presented in Table 1. Consistent with the previous literature, all of the residues contained excess scrubber in the form of $Ca(OH)_2$ and some $CaCO_3$ resulting from absorption of CO_2 in the flue gases and during storage. Although no DTA response per %w/w $Ca(OH)_2$ calibration curve could be established for residue A3 (Appendix A), comparison of the DTA peak area with calibration curves determined for the other residues showed a maximum $Ca(OH)_2$ concentration of 0.75%w/w. This concentration was therefore used to calculate the CaClOH content of the residue. The very low $Ca(OH)_2$ and high $CaCO_3$ concentration observed for residue A3 is believed to be a result of carbonation during the storage of the residue because flue gases would typically not contain more than ~10% volume CO_2 (Bodenan and Deniard 2003; Jacquinot et al. 2000). Residue A3 also contained chlorocalcite ($KCaCl_3$) which has previously been observed in carbonated APC residue and attributed to a complex carbonation reaction of the CaClOH phase in the presence of KCl (Wang et al. 2010). Carbonation of APC residues prior to treatment may not be a consistent occurrence but has significant implications for the properties of the residues (Baciocchi et al. 2009; Cappai et al. 2012; Li et al. 2007; Wang et al. 2010). Unless care is taken to control the process, carbonation will provide another mechanism by which residue characteristics and therefore behaviour will vary. The $CaCO_3$ concentration in residue A5 could not be determined by thermogravimetric analysis. This residue showed a very large mass loss in the range associated with $CaCO_3$ decomposition despite showing relatively little evidence of calcite by XRD. The mass loss observed by TGA was therefore believed to be associated with volatisation of the high concentration of chloride salts in addition to the decomposition of the calcite (Chen et al. 2012).

The residues contained varying concentrations of alkali metal chlorides and $CaSO_4$ resulting from the neutralisation of SO_X gases (Figure 1)(Bodenan and Deniard 2003). Such variations are reflected in the water soluble Cl and SO_4 salt content of the residues, which comprise the large majority of the water soluble fraction (Table 1). Water soluble Cl and SO_4 concentrations (at l/s=10) covered ranges similar to those which can be observed when comparing results reported throughout previous literature (Cl: 96,300-~500,000 mg/kg; SO_4: 7000-20,490 mg/kg) (Baciocchi et al. 2009; Cappai et al. 2012; Geysen et al. 2004b; Lampris et al. 2009; Li et al. 2007; Quina et al. 2008b).

Figure 1 XRD patterns for as-received residues and matched reference patterns (maximum peak intensities of sample patterns normalised)

The mineralogical variability of the residues also had implications for their respective ANC and pH buffering behaviour. ANC was largely associated with the excess alkaline scrubber. This is reflected when comparing the concentration of $Ca(OH)_2$+$CaCO_3$ with the ANC to pH 4.5 (presented as $CaCO_3$ equivalent in Table 1), and in the pH of the predominant buffering plateaus (Figure 2) which are associated with these compounds. However, additional pH buffers must be present to account for the capacity displayed by residue A5 and the discrepancy between the measured and theoretical capacities based on quantification of $Ca(OH)_2$ and $CaCO_3$ concentrations by thermal analysis. Additional buffering may be attributable to precipitation of $Ca(OH)_2$ following dissolution of the CaClOH phase. Previous analysis of semi-dry APC residues throughout the literature has shown similar qualitative behaviour and greater variability to that observed in the current study with ANC to pH 4.5 between 4.5-16mEq/g (22.5-80%$CaCO_3$ equivalent) (Astrup et al. 2006; Baciocchi et al. 2009; International Ash Working Group 1997).

The ANC of the clinical waste residue (A1), was much greater than the MSWI residues which coincided with the large excess of $Ca(OH)_2$ (Table 1). Clinical or hospital wastes typically contain greater concentrations of PVC and therefore HCl in the gas stream (Jacquinot et al. 2000). Greater concentration of alkaline scrubber may therefore be injected. To ensure emissions limits were complied with, the facility from which residue A1 was collected did not re-circulate the scrubber residue. However, large quantities of excess scrubber do not appear to necessarily be associated with hospital or clinical waste incinerator residues. Some previous studies have observed very little excess scrubber in hospital waste APC residues (Bodenan and Deniard 2003; Kougemitrou et al. 2011) whilst MSW APC residues have been observed to contain large quantities (Bodenan and Deniard 2003; Geysen et al. 2004a).

Figure 2 ANC curves for as-received residues

3.2 Characterisation and performance of S/S products

3.2.1 Engineering properties (workability, setting time, compressive strength, bulk porosity)

Working with a constant mix design, a very broad range of workability was observed for the five residues studied (Table 2). Stegemann and Zhou (Stegemann and Zhou 2009) suggested a flow table spread of >~175mm to be suitable for s/s applications. Samples containing residue A5 were therefore considered excessively stiff. Samples containing residues A2 and in particular A3 showed particularly high flow values suggesting a lower liquid to solid ratio would be beneficial to improve the ease of handling and placing, and optimise other properties such as compressive strength and permeability (Neville and Brooks 1994). Flow values were strongly correlated with the specific surface area of the residues suggesting this to be an important determining factor, consistent with previous literature regarding supplementary cementitious materials (Quercia et al. 2012; Walker and Pavia 2011). However, the specific surface area of the residues after blending for s/s would vary from that observed when testing the as-received residues due to dissolution of a proportion of the water soluble content in the liquid phase. APC residues can also chemically incorporate as well as adsorb water due to the mineralogy e.g. hydration of anhydrite to form gypsum. The water demand of the blends and consequently flow value observed may therefore also be affected by the differing mineralogy of the samples.

Table 2 Workablity, setting time, 28 day compressive strength with and without 7 days submersion in de-ionised water (7d sub), bulk porosity after 28 days, and concentration of $Ca(OH)_2$ and $CaCO_3$ in 28 day

old samples determined by STA. Nomenclature 2:3 AX indicates the waste:binder ratio and residue incorporated. >=greater than testable by flow table.

Residue variability also strongly influenced the reaction kinetics observed by isothermal conduction calorimetry (Figure 3). All blends showed an acceleration of the cement hydration kinetics due to the high concentration of chloride salts present in the residues (Kondo et al. 1977; Taylor 1997). The acceleratory effect was observed to be greater when including residues with higher Cl concentrations. Acceleration in blends containing residues A1 and A5 (those with the highest soluble Cl content (Table 1)) was sufficient to remove the induction period such that the heat flow maximum associated with tricalcium silicate (C_3S) hydration could not be fully distinguished from the initial exotherm associated with wetting of the cement, and hydration of free lime and calcium sulphates (Bensted 1987). Ramachandran showed tricalcium silicate hydration to accelerate with addition of up to 20% $CaCl_2$ by weight of C_3S (Ramachandran 1976). According to the concentrations of Cl presented in Table 1 and the mix designs applied, sample 2:3 A5 would contain a Cl concentration equivalent to 37.5% $CaCl_2$ by weight of C_3S (assuming C_3S content of the cement to be 65%w/w (Herfort et al. 2010)). However, chlorides are present as a range of salts in APC residues, and additional non-chloride salts are also present. This complexity would cause variation from the behaviour observed in the purer blends studied by Ramachandran (Kondo et al. 1977; Wilding et al. 1984).

CEM I hydration shows a second heat evolution peak ~16 hours, attributed to dissolution of the tricalcium aluminate phase and precipitation of ettringite (Jansen et al. 2012). When blended with the APC residues the second peak is only clearly visible for samples 2:3 A3 and 2:3 A4. These samples contained the residues with the highest soluble sulphate concentrations (Table 1). For sample 2:3 A4 the second peak is very low, however, for sample 2:3 A3 the two peaks are clearly resolved. Further investigations are required to investigate and explain the effects of this residue on the cement hydration kinetics.

Figure 3 Heat flow (normalised to mass of CEM I) for samples prepared with a waste:binder ratio=2:3 incorporating residues A1-A5, and a neat CEM I paste. All samples prepared at l/s=0.5.

Setting times of cementitious matrices are determined by the hydration kinetics together with the interparticle spacing of the pastes (Bentz et al. 2009). Workability is also largely a result of the interparticle spacing, or volume fraction of solids in suspension, and therefore often shows correlation with setting time (Lampris et al. 2008; Lampris et al. 2009). Initial and final setting times for the s/s products are shown in Table 2. Consistent with the accelerated reaction kinetics and low flow values observed (Figure 3 and Table 2 respectively) samples 2:3 A1 and 2:3 A5 showed the shortest setting times. Samples containing residues A3 and A4 surpassed the minimum recommended time for initial setting of ~2 hours in order to allow time to cast/place the mixture (Stegemann and Zhou 2009). Samples containing residues A1, A2 and A5, suffered excessively rapid initial setting times. All samples met final set within the recommended upper limit of ~24 hours.

Twenty-eight day compressive strength and bulk porosity showed little variation (Table 2) suggesting the residue variability played a negligible role in determining these properties. All samples met the one MPa minimum value for compressive strength required by European waste acceptance criteria for monolithic waste forms (EC 2003). Generally samples showed a slight increase in the compressive strength following the seven day submersion procedure recommended by Stegemann and Zhou (Stegemann and Zhou 2009), which may be associated with increased cement hydration. Sample 2:3 A5 showed a decrease in compressive strength. This is believed to be associated with the greater soluble solids content present in this product (indicated in Table 3 by the TDS observed as a result of granular leach testing) and therefore the greater loss of material through leaching upon submersion. This process would leave voids within the product and consequently reduce the compressive strength, overcoming any potential increase due to hydration. Lampris et al observed an increase in compressive strength as a result of the same submersion procedure when working with APC residue/cement blends at low waste:binder ratios, and a decrease at high waste:binder ratios, similarly showing that the compressive strength development is dependent on the availability of soluble solids within the matrices (Lampris et al. 2009). Dyer (2010) also acknowledged the potential for Portland cement based s/s products to gain compressive strength during leaching procedures and showed development to be associated with the progression of the leached zone through the monolith, again relating compressive strength development to the extent of materials loss (Dyer 2010).

3.2.2 Leaching behaviour, mineralogy and ANC

Consistent with previous work examining the incorporation of APC residues into cementitious matrices, chloride release and TDS during granular leach testing surpassed hazardous WAC limits (25,000 mg/kg and 100,000 mg/kg respectively) (Lampris et al. 2008; Lampris et al. 2009; Shirley and Black 2011b) (Table 3). Samples 2:3 A2 and 2:3 A4 showed TDS slightly below the limit, primarily as a result of incidental dilution. Although the behaviour of all products was similar with regards to compliance with WAC, the magnitude of chloride release and TDS varied depending on the residue used and spanned a factor of approximately two in both cases.

Table 3 Table 4 Granular (BS EN 12457-2) and monolithic (EA NEN 7375) leach test results for the s/s products tested after 28 days curing. ε^*_{64}=Measured cumulative release over 64 days

Chlorides were revealed by XRD analysis (Figure 4) to be present as NaCl and KCl in varying proportions which were observed to be removed upon leach testing. However, reflections for both phases were of very low intensity in all samples, suggesting low concentrations. Analysis by XRD also revealed chlorides to be present in the AFm phases. Broad reflections close to those characteristic of Friedel's salt were observed in all samples, and sample 2:3 A5 showed evidence of the Kuzel's salt phase. The variability observed in the composition of the AFm phases can be attributed to the sensitivity of these phases to the local chemical environment and their ability to incorporate a range of ions depending on the relative availabilities (Glasser et al. 1999; Matschei et al. 2007). Chlorides bound within the AFm phases are largely retained during leach testing (Shirley and Black 2011a). Considering the high release of chlorides observed (Table 3) and the minimal evidence for chlorides within soluble crystalline compounds, it seems likely that a significant proportion of the chlorides were present within the amorphous fraction of the products. Chlorides were perhaps sorbed onto the C-S-H phase in which instance they would remain predominantly water soluble (Beaudoin et al. 1990) explaining the high mobility observed.

In addition to showing variability in the composition of the AFm phases present, variable composition of the AFt phases was observed. Samples containing residues A1 and A5, which contained the lowest soluble sulphate concentrations (Table 1), showed a clear shift in the Bragg angle of the reflections associated with the AFt phase (Figure 4), indicating substitution in the ettringite structure (Poellmann et al. 1990). Low angle reflections for samples 2:3 A1 and 2:3 A5 were a good match for the AFt phase containing OH ions. However, this phase is reportedly unstable, carbonating readily (Taylor 1997). It seems likely however that due to the availability of the various anions, some level of sulphate substitution with OH and CO_3 ions has occurred. Cl substituted ettringite is reportedly unstable above 0°C and was therefore considered unlikely to be present (Taylor 1997). No sulphate release was observed from any of the matrices with detection limits of 2ppm (20 mg/kg) following dilution for analysis, indicating that WAC limits concerning sulphates were not a concern.

Figure 4 XRD patterns for s/s products recorded after 28 days curing (y scales adjusted for clarity) and matched reference patterns

Mineralogical differences were also observed as varying concentrations of $Ca(OH)_2$ and $CaCO_3$ in the products (Table 2 and Figure 4). The concentration of $Ca(OH)_2$ in the matrices would depend on both the concentration initially present in the residue and the extent of cement hydration. Concentrations presented in Table 2 were determined by STA and were also reflected in the ANC of the products (Figure 5). Ranking of the products according to the ANC to pH 7 showed a similar order to the ranking of the as-received residues (Figure 2), suggesting that the differences in buffering at alkaline pH values was predominantly a result of the alkalinity of the residues rather than differences in the concentration of cement reaction products. Other than residue A1, all of the products showed greater alkaline buffering than the as-received residues due to the alkaline products of cement hydration. Considerable differences in the ANC of the s/s products would be particularly important for the long-term mobility of metal contaminants, the solubility of which is highly pH dependant (Stegemann and Zhou 2009). Leaching of metals was not studied as part of the current work but would be necessary for a comprehensive assessment of the suitability of a treatment option.

Figure 5 ANC curves for s/s products cured for 28 days

Although the alkalinity of the samples was variable, pH conditioning during leaching tests varied very little regardless of the residue incorporated in the products (Table 3 and Figure 6). pH measured in the early fractions of the monolithic leach test was ~11.8-12.2 whilst that of latter fractions rose to ~12.5 (Figure 6). This behaviour can be attributed to the dissolution of $Ca(OH)_2$ coupled with the very high release of calcium chloride compounds during the initial fractions, which would lower the pH of a saturated $Ca(OH)_2$ or cement matrix solution (Tritthart 1989; Tuddenham and Anderson 1950). Chloride release from all samples occurred via a depletion controlled mechanism according to analysis by EA NEN 7375 (based on the gradient of plots in Figure 7). Despite the similar mechanism controlling release, the magnitude of release (ε^*_{64} presented in Table 3), varied by as much as 490,000 mg/m^2. Consistent with previous work (Lampris et al. 2008; Lampris et al. 2009; Shirley and Black 2011b), all samples surpassed monolithic hazardous WAC limits for Cl of 20,000 mg/m^2. Following completion of the test compressive strength of the monoliths was measured (Table 3). All of the samples except for 2:3 A5 gained compressive strength as a result of exposure to water, showing similar behaviour to that observed during the shorter seven day submersion procedure.

Figure 6 pH conditioned by s/s products during EA NEN 7375:2004

Figure 7 Plots used to determine Cl release mechanisms from s/s products (by gradient analysis) according to EA NEN 7375:2004

4 Conclusions and Practice Relevance

APC residues are an inherently variable waste stream. This variability has significant implications for the behaviour of products produced by s/s and should be considered when researching or applying management options. Any technical treatment is likely to require modification in order to successfully handle a specific residue batch. The current work has demonstrated this by examining the implications of variability across five batches of APC residue collected from different UK EfW facilities for treatment by s/s, using cement as a binder. Differences in the residues' mineralogy and morphology resulted in clear differences in properties of the s/s products including workability, reaction kinetics, setting time and the magnitude of chloride release during regulatory testing. Mineralogy of the products also varied. In particular, this was observed with regards to the composition of the AFm and AFt minerals, the concentration of $Ca(OH)_2$ and $CaCO_3$, and consequently the acid neutralisation capacity of the s/s products. Other important properties of the products such as compressive strength, bulk porosity and the mechanism controlling chloride release were observed to be largely independent of the properties of the residue incorporated.

5 Acknowledgements

This research was funded by an EPSRC CASE award 07002463

References

Alba N, Vazquez E, Gasso S and Baldasano JM (2001) Stabilization/solidification of MSW incineration residues from facilities with different air pollution control systems. Durability of matrices versus carbonation. *Waste Management,* **21(4)**: 313-323.

Amutha Rani D, Boccaccini AR, Deegan D and Cheeseman CR (2008) Air pollution control residues from waste incineration: Current UK situation and assessment of alternative technologies. *Waste Management,* **28(11)**: 2279-2292.

Astrup T, Jakobsen R, Christensen TH, Hansen JB and Hjelmar O (2006) Assessment of long-term pH developments in leachate from waste incineration residues. *Waste Management & Research,* **24(5)**: 491-502.

Baciocchi R., Costa G, Di Bartolomeo E, Polettini A and Pomi R (2009) The effects of accelerated carbonation on CO_2 uptake and metal release from incineration APC residues. *Waste Management,* **29(12)**:2994-3003.

Beaudoin JJ, Ramachandran VS and Feldman RF (1990) Interaction of chloride and C-S-H. *Cement and Concrete Research,* **20(6)**: 875-883.

Bensted J (1987) Some applications of conduction calorimetry to cement hydration. *Advances in Cement Research,* **1(1)**: 35-44.

Bentz DP, Peltz MA and Winpigler J (2009) Early-age properties of cement-based materials: II. Influence of water-to-cement ratio *ASCE Journal of Materials in Civil Engineering,* **21(9)**: 512-517.

Bodenan F and Deniard P (2003) Characterization of flue gas cleaning residues from European solid waste incinerators: Assessment of various Ca-based sorbent processes. *Chemosphere,* **51(5)**: 335-347.

Cappai G, Cara S, Muntoni A and Piredda M (2012) Application of accelerated carbonation on MSW combustion APC residues for metal immobilization and CO_2 sequestration. *Journal of Hazardous Materials,* **207**: 159-164.

Chen WS, Chang FC, Shen YH, Tsai MS and Ko CH (2012) Removal of chloride from MSWI fly ash. *Journal of Hazardous Materials,* **237**: 116-120.

De Boer JH, Lippens BC, Linsen BG *et al.* (1966) T-Curve of Multimolecular N_2-Adsorption. *Journal of Colloid and Interface Science,* **21(4)**: 405-&.

De Boom A and Degrez M(2012) Belgian MSWI fly ashes and APC residues: A characterisation study. *Waste Management,* **32(6)**: 1163-1170.

Dean JA and Lange NA (1999) *Lange's handbook of chemistry,* 15th ed. McGraw-Hill, New York, USA

Dyer TD (2010) Modification of strength of wasteforms during leaching. *Proceedings of the ICE - Waste and Resource Management,* **163**: 111-122.

Dyer TD, Halliday JE and Dhir RK (2006) Influence of solid solutions on chloride leaching from wasteforms. *Proceedings of the ICE - Waste and Resource Management,* **159**: 131-139.

EC (2003) Council decision 2003/33/EC establishing criteria and procedures for the acceptance of waste at landfills pursuant to Article 16 of and Annex II to Directive 1999/31/EC. *Official Journal of the European Communities,* **L11**: 27-49.

EC (2006) Directive 2006/118/EC on the protection of groundwater against pollution and deterioration. *Official journal of the European communities,* **L372/19**.

EC (2008) Council directive 2008/98/EC of the European Parliament and of the Council of 19 November 2008 on waste and repealing certain directives. *Official journal of the European union,* **L312**: 3-30.

EC (2010) Directive 2010/75/EU of the European Parliment and of the Council, on industrial emissions (integrated pollution prevention and control) (recast). *Official Journal of the European Union,* **L 334**: 17-119.

Environment Agency (2002) *Solid residues from municipal waste incinerators in England and Wales*.

Geysen D, Imbrechts K, Vandecasteele C, Jaspers M and Wauters G (2004a) Immobilization of lead and zinc in scrubber residues from MSW combustion using soluble phosphates. *Waste Management,* **24(5)**: 471-481.

Geysen D, Vandecasteele C, Jaspers M and Wauters G (2004b) Comparison of immobilisation of air pollution control residues with cement and with silica. *Journal of Hazardous Materials,* **107(3)**: 131-143.

Glasser FP, Kindness A and Stronach SA (1999) Stability and solubility relationships in AFm phases - Part 1. Chloride, sulfate and hydroxide. *Cement and Concrete Research,* **29(6)**: 861-866.

Herfort DG, Moir K, Johansen V, Sorrentino F and Arceo HB (2010) The chemistry of Portland cement clinker. *Advances in Cement Research,* **22**: 187-194.

International Ash Working Group (1997) *Municipal solid waste incinerator residues.* Elsevier, Amsterdam, Netherlands

Jacquinot B, Hjelmar O and Vehlow J (2000) *The influence of PVC on the quantity and hazardousness of flue gas residues from incineration.* Bertin technologies report, available online at http://ec.europa.eu/environment/waste/studies/pvc/incineration.pdf.

Jansen D, Goetz-Neunhoeffer F, Lothenbach B and Neubauer J (2012) The early hydration of Ordinary Portland Cement (OPC): An approach comparing measured heat flow with calculated heat flow from QXRD. *Cement and Concrete Research,* **42(1)**: 134-138.

Kondo R, Daimon M, Sakai E and Ushiyama H (1977) Influence of inorganic salts on hydration of tricalcium silicate. *Journal of Applied Chemistry and Biotechnology,* **27(4)**: 191-197.

Kougemitrou I, Godelitsas A, Tsabaris C *et al.* (2011) Characterisation and management of ash produced in the hospital waste incinerator of Athens, Greece. *Journal of Hazardous Materials,* **187(1-3)**: 421-432.

Lampris C, Stegemann JA and Cheeseman CR (2008) Chloride leaching from air pollution control residues solidified using ground granulated blast furnace slag. *Chemosphere,* **73(9)**: 1544-1549.

Lampris C, Stegemann JA and Cheeseman CR (2009) Solidification/stabilisation of air pollution control residues using Portland cement: Physical properties and chloride leaching. *Waste Management,* **29(3)**: 1067-1075.

Lampris C, Stegemann JA, Pellizon-Birelli M, Fowler GD and Cheeseman CR (2011) Metal leaching from monolithic stabilised/solidified air pollution control residues. *Journal of Hazardous Materials,* **185(2-3)**: 1115-1123.

Li XM, Bertos MF, Hills CD, Carey PJ and Simon S (2007) Accelerated carbonation of municipal solid waste incineration fly ashes. *Waste Management,* **27(9)**: 1200-1206.

Matschei T, Lothenbach B and Glasser FP (2007) The AFm phase in Portland cement. *Cement and Concrete Research,* **37(2)**: 118-130.

Neville AM and Brooks JJ (1994) *Concrete technology.* 2nd (revised) ed. Longman Scientific and Technical, Harlow, UK

Poellmann H, Kuzel HJ and Wenda R (1990) Solid-solution of ettringites. 1. Incorporation of OH- and CO_3^{2-} in $3CaO$-Al_2O_3-$3CaSO_4$-$32H_2O$. *Cement and Concrete Research,* **20(6)**: 941-947.

Quercia G, Husken G and Brouwers HJH (2012) Water demand of amorphous nano silica and its impact on the workability of cement paste. *Cement and Concrete Research,* **42(2)**: 344-357.

Quina MJ, Bordado JC and Quinta-Ferreira RM (2008a) Treatment and use of air pollution control residues from MSW incineration: An overview. *Waste Management,* **28(11)**: 2097-2121.

Quina MJ, Santos RC, Bordado JC and Quinta-Ferreira RM (2008b) Characterization of air pollution control residues produced in a municipal solid waste incinerator in Portugal. *Journal of Hazardous Materials,* **152(2)**: 853-869.

Ramachandran VS (1976) *Calcium Chloride in Concrete.* Applied Science Publishers.

Rouquérol F, Rouquerol J and Sing KSW (1999) *Adsorption by Powders and Porous Solids: Principles, Methodology and Applications.* Academic Press, London, UK

Shirley R and Black L (2011a) Alkali activated solidification/stabilisation of air pollution control residue using co-fired PFA: mineralogical characterisation. *Advances in Applied Ceramics,* **110(8)**: 438-445.

Shirley R and Black L (2011b) Alkali activated solidification/stabilisation of air pollution control residues and co-fired pulverised fuel ash. *Journal of Hazardous Materials,* **194**: 232-242.

Sing KSW (1982) Reporting Physisorption data for gas solid systems- with special reference to the determination of surface-area and porosity. *Pure and Applied Chemistry,* **54(11)**: 2201-2218.

Stegemann JA and Zhou Q (2009) Screening tests for assessing treatability of inorganic industrial wastes by stabilisation/solidification with cement. *Journal of Hazardous Materials,* **161(1)**: 300-306.

Taylor H (1997) *Cement chemistry.* 2nd ed. Thomas Telford, London, UK

Tritthart J (1989) Chloride binding in cement. 2. The influence of the hydroxide concentration in the pore solution of hardened cement paste on chloride binding. *Cement and Concrete Research,* **19(5)**: 683-691.

Tuddenham WM and Anderson DH (1950) Buffer for High pH Measurements. *Analytical Chemistry,* **22(9)**: 1146-1148.

UK Statutory Instruments (2005) 1640 of 16th July 2005, The Landfill (England and Wales) (Amendment) Regulations 2005.

UK Statutory Instruments (2010) 675 of 10th March 2010, The Environmental Permitting (England and Wales) Regulations 2010.

Walker R and Pavia S (2011) Physical properties and reactivity of pozzolans, and their influence on the properties of lime-pozzolan pastes. *Materials and Structures,* **44(6)**: 1139-1150.

Wang L, Jin YY and Nie YF (2010) Investigation of accelerated and natural carbonation of MSWI fly ash with a high content of Ca. *Journal of Hazardous Materials,* **174(1-3)**: 334-343.

Wilding CR, Walter A and Double DD (1984) A classification of inorganic and organic admixtures by conduction calorimetry. *Cement and Concrete Research,* **14(2)**: 185-194.

Williams PT (2005) *Waste Treatment and Disposal.* 2nd ed. Wiley, Chichester, UK

Young JR, How MJ, Walker AP and Worth WMH (1988) Classification as corrosive or irritant to skin of preparations containing acidic or alkaline substances, without testing on animals. *Toxicology in Vitro,* **2(1)**: 19-26.

Figure 1

Click here to download high resolution image

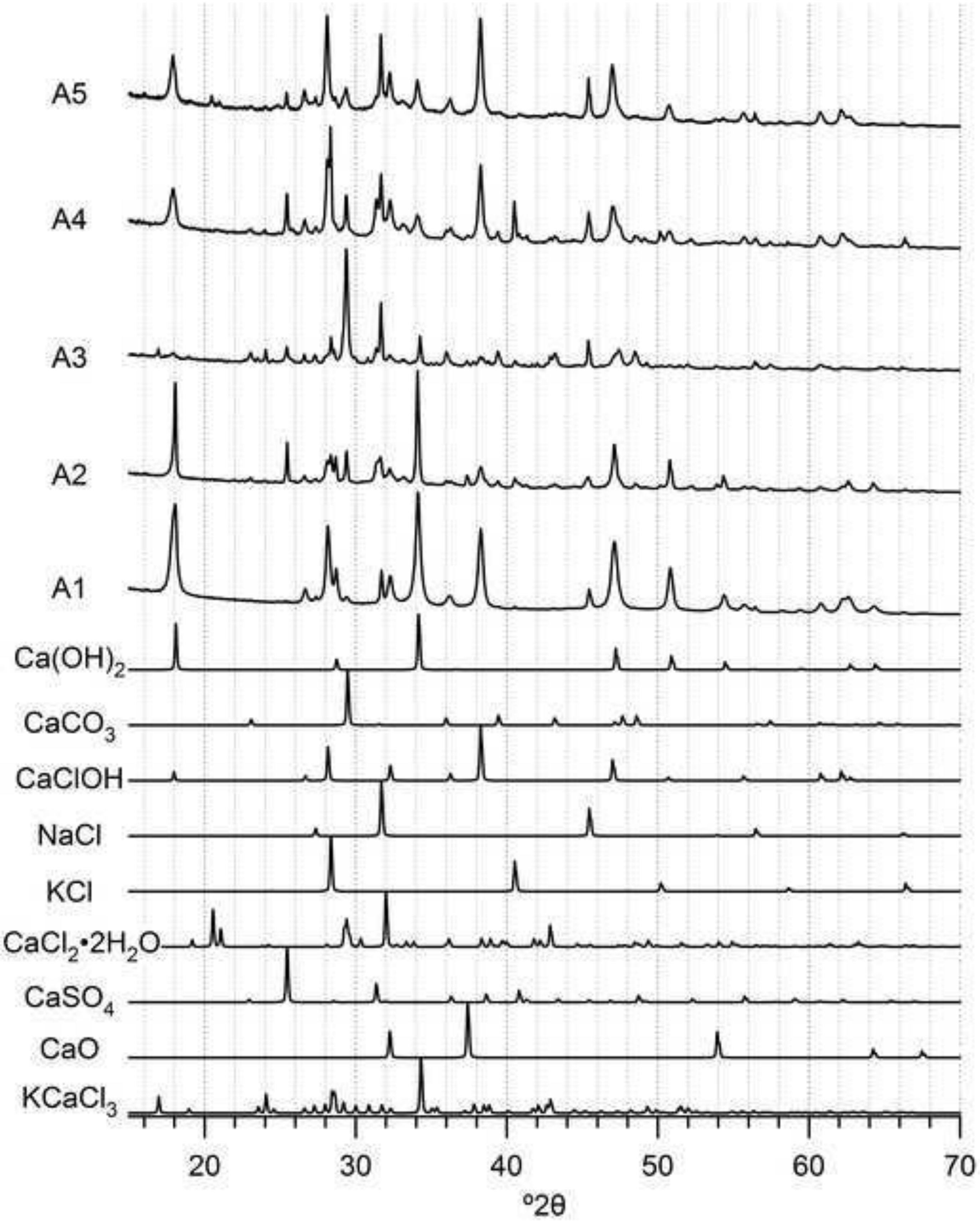

Figure 2

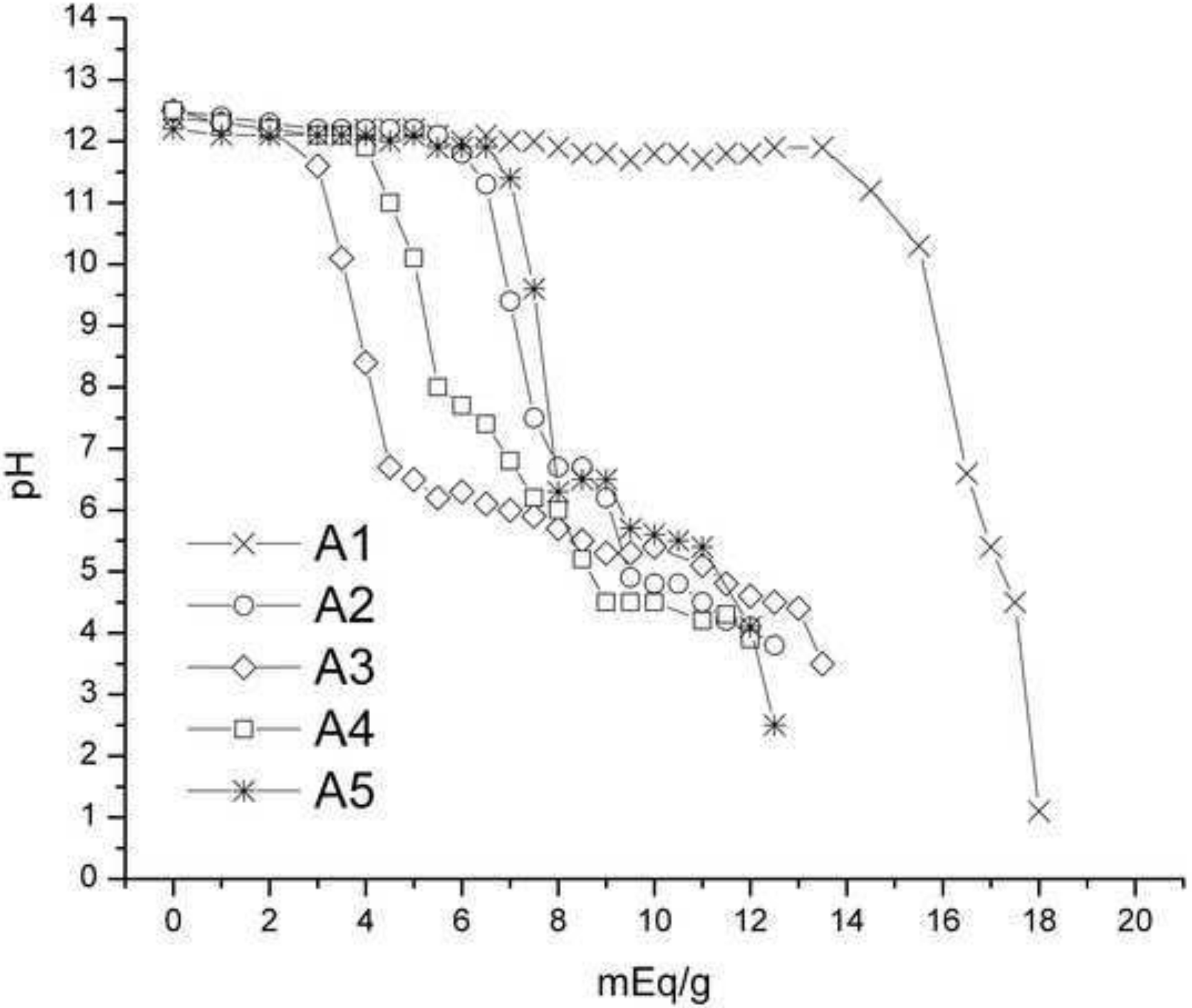
pH
mEq/g
0
1
2
3
4
5
6
7
8
9
10
11
12
13
14
0
2
4
6
8
10
12
14
16
18
20
A1
A2
A3
A4
A5

Figure 3

Click here to download high resolution image

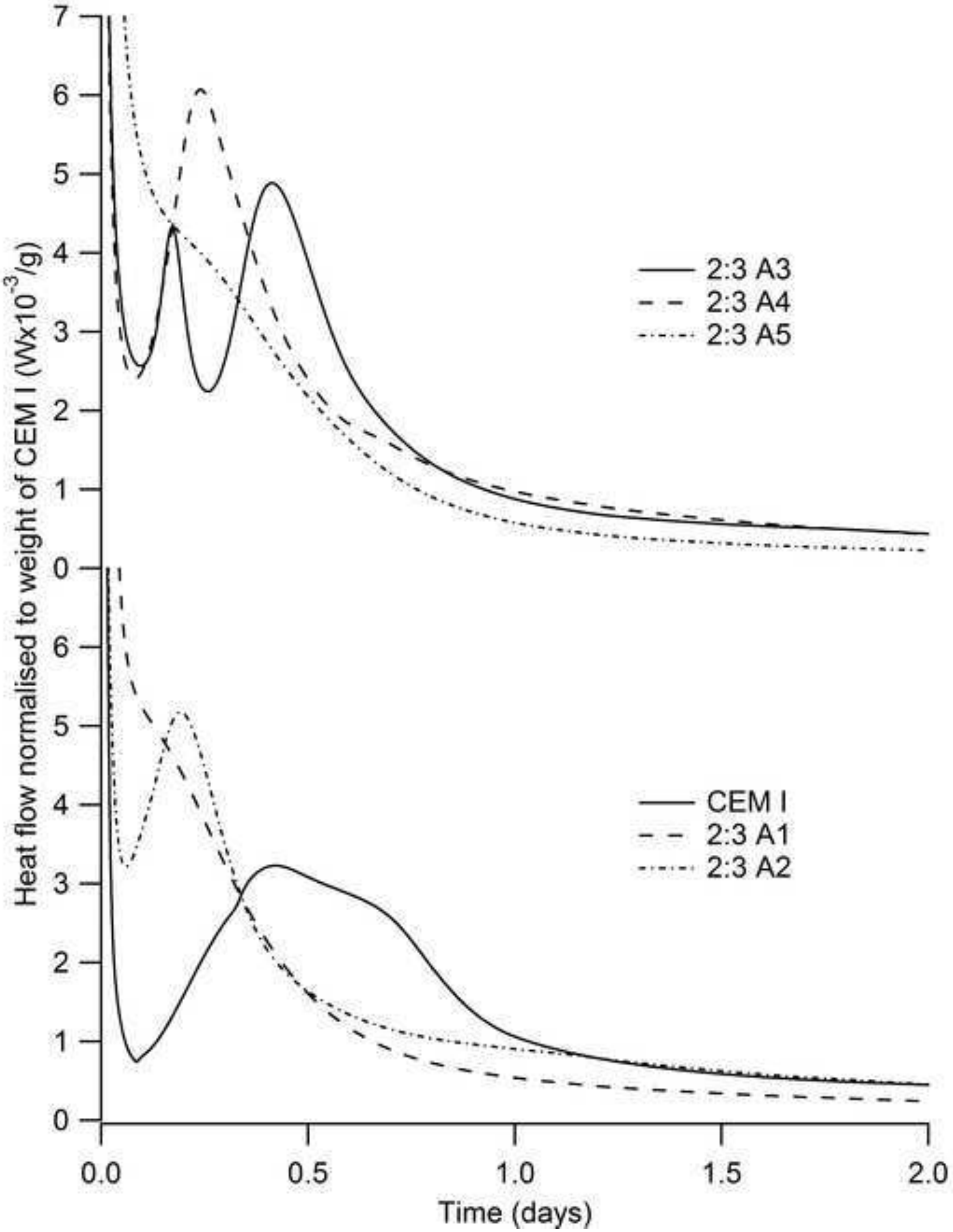

Figure 4
Click here to download high resolution image

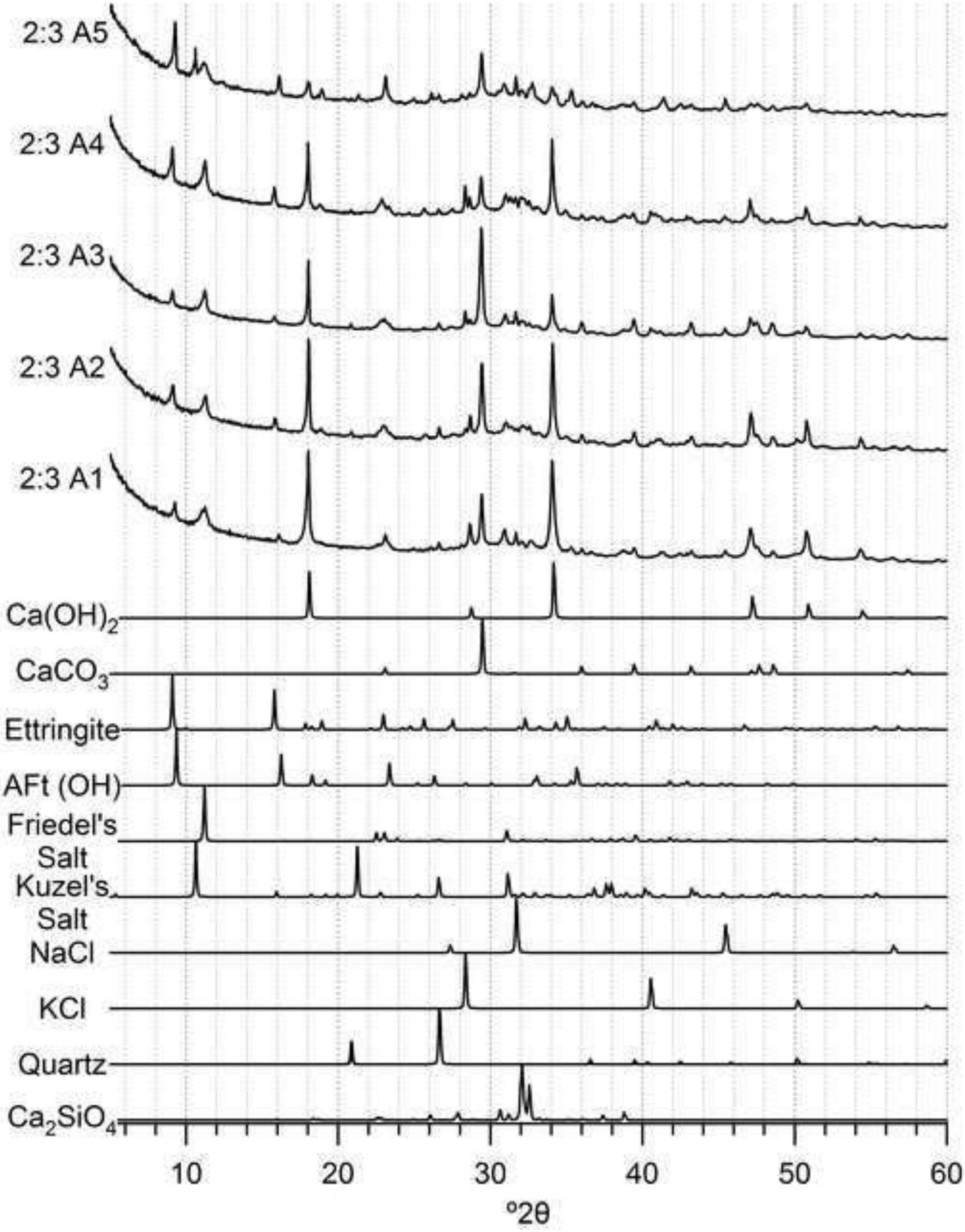

Figure 5

Click here to download high resolution image

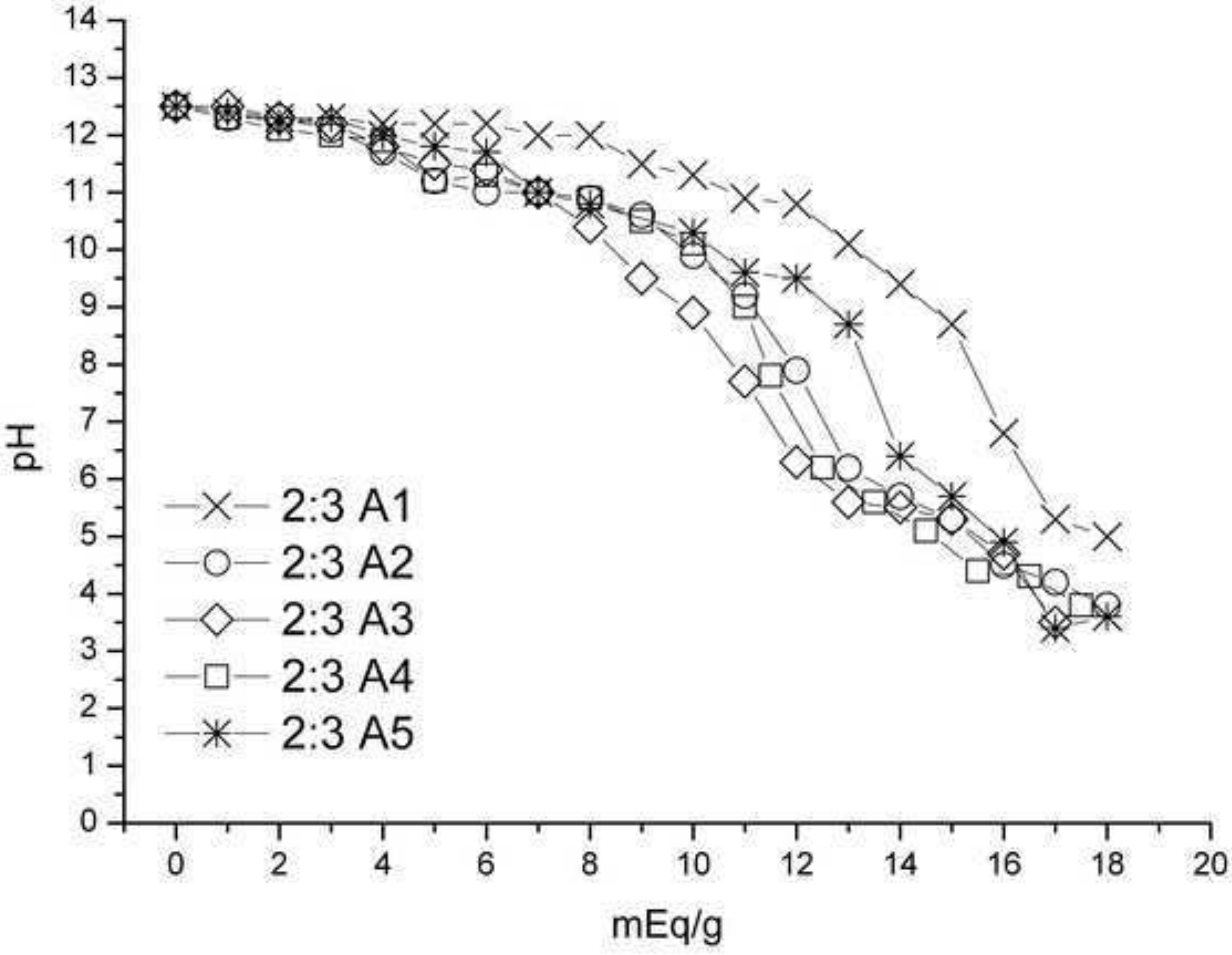

Figure 6

Click here to download high resolution image

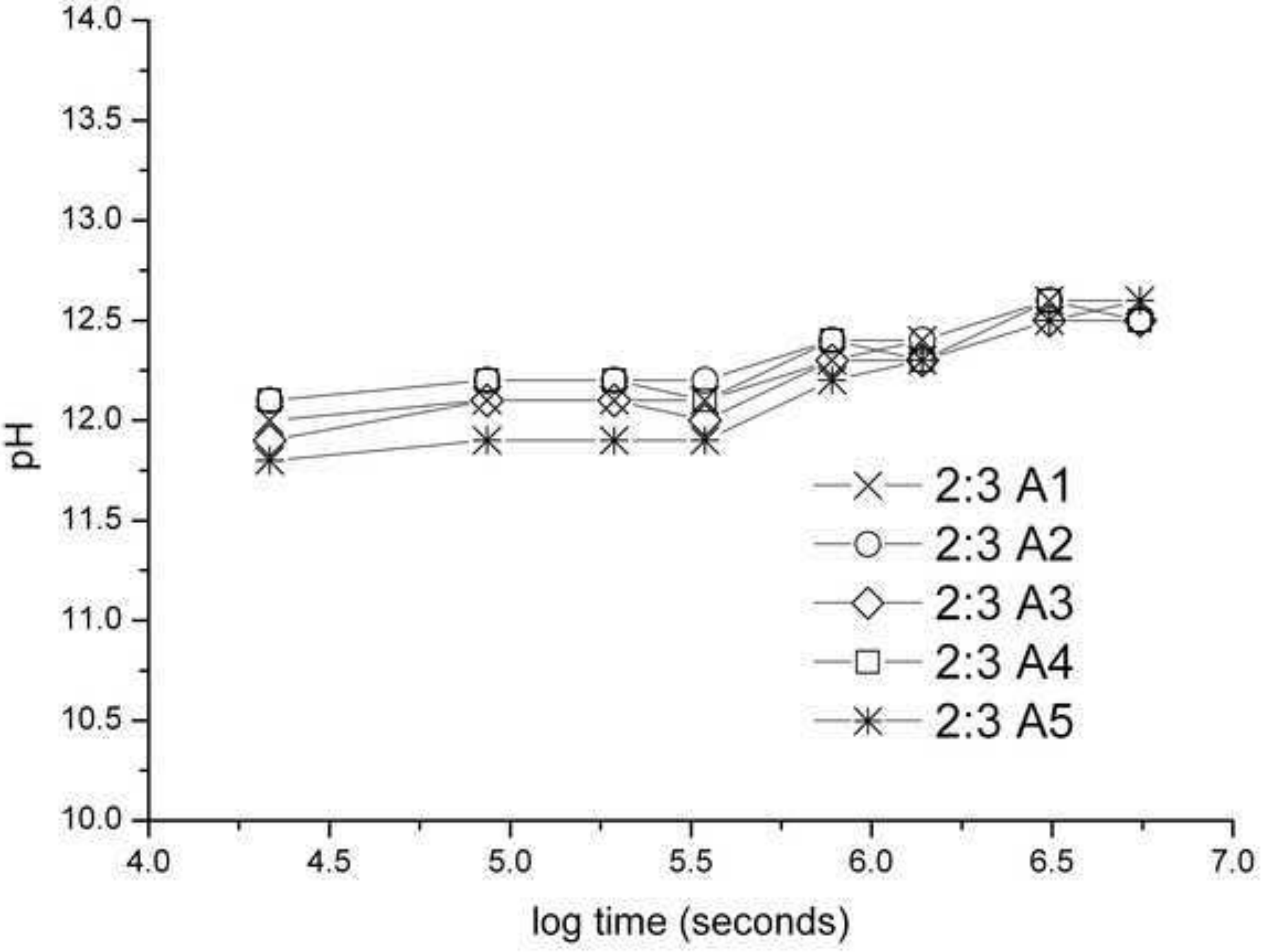

Figure 7

Click here to download high resolution image

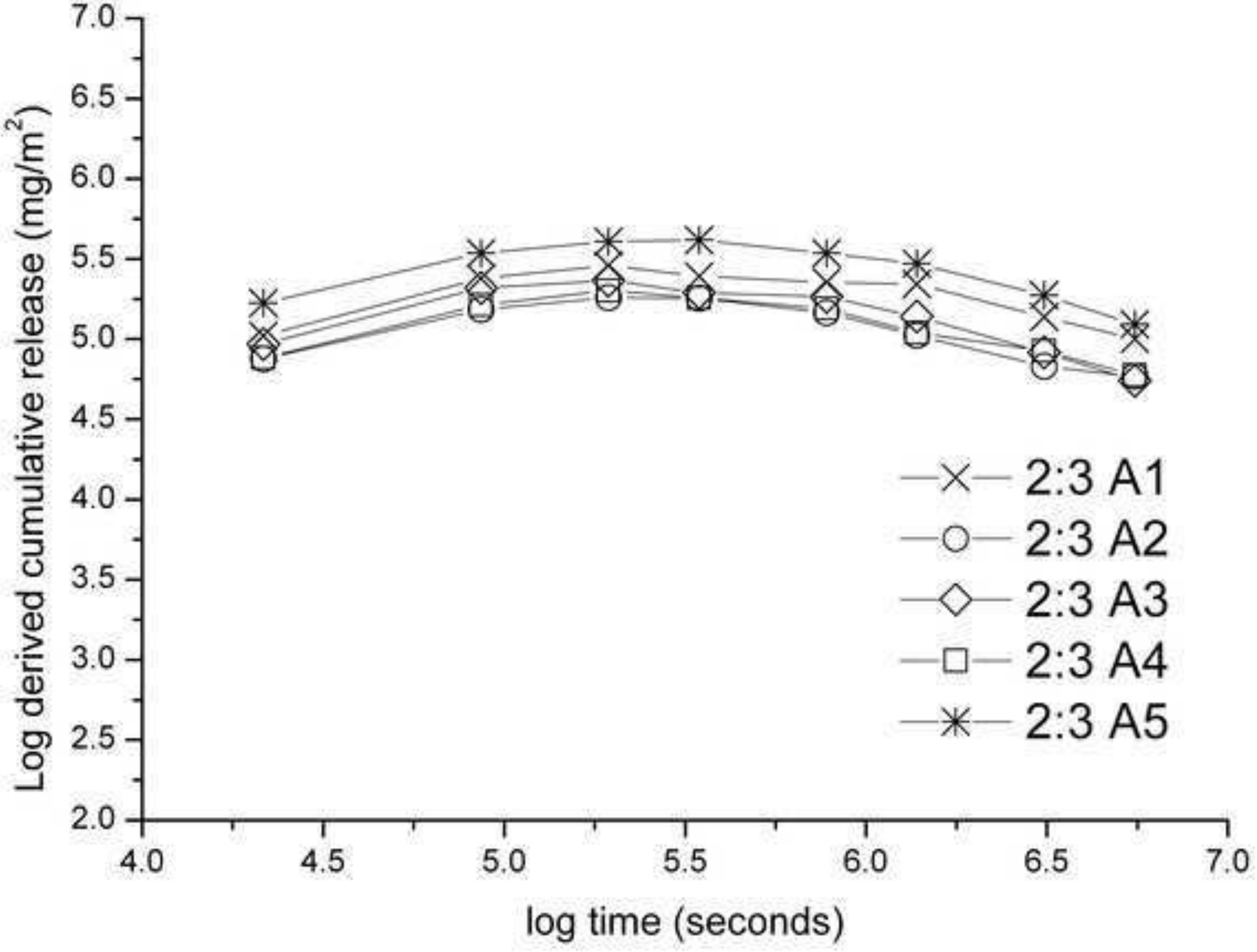

	A1	A2	A3	A4	A5
Cl (mg/kg)	157,400	105,300	132,400	112,600	233,600
SO_4 (mg/kg)	3500	8500	11,800	12,300	5700
TDS (mg/kg)	333,300	235,100	304,700	271,800	460,500
pH	12.4	12.5	12.4	12.5	12.2
Alkalinity (%$CaCO_3$ $_{\text{equiv}}$)	87.5	55	62.5	50	58.5
$Ca(OH)_2$ (%w/w_{dry})	34.4	11.6	0.8	3.9	4.0
CaClOH (%w/w_{dry})	23.5	17.8	13.8	15.1	5.8
$CaCO_3$ (%w/w_{dry})	4.4	7.3	28.6	10.3	nd.
Density (kg/m^3)	2200	2400	2600	1900	2200
BET ‘C’ value	134.9	192.4	158.2	278.8	467.5
BET surface area (m^2/g)	7.4	4.5	1.9	6.1	21.8
Micropore area (m^2/g)	0.9	0.8	0.3	1.4	6.3
External Surface area (m^2/g)	6.5	3.7	1.6	4.7	15.4

Table 1 Analysis of as-received residues including pH and release of Cl, SO_4 and TDS during BS EN 12457-2, alkalinity to pH 4.5 presented as %$CaCO_3$ equivalent, concentration of compounds evident from STA (%w/w_{dry}), density and specific surface area determined by N_2 sorption isotherms.

	2:3 A1	2:3 A2	2:3 A3	2:3 A4	2:3 A5
Flow Value (mm)	190	205	>	195	145
Initial Setting Time (h)	0.3	1.7	5.5	5.2	0.1
Final Setting Time (h)	0.7	3.5	5.9	5.5	0.2
28 day UCS (MPa)	10.2 ± 2.3	10.5 ± 0.5	10.2 ± 0.9	10.2 ± 0.2	11.3 ± 0.2
UCS (7d sub) (MPa)	11.3	15.2	14.4	10.7	9.0
Porosity (%)	45.4	44.2	47.2	45.6	40.3
28 day $Ca(OH)_2$ (%w/w_{dry})	20.6	11.8	8.7	9.3	7.2
28 day $CaCO_3$ (%w/w_{dry})	8.8	10.8	18.8	5.2	10.8

Table 2 Workablity, setting time, 28 day compressive strength with and without 7 days submersion in de-ionised water (7d sub), bulk porosity after 28 days, and concentration of $Ca(OH)_2$ and $CaCO_3$ in 28 day old samples determined by STA. Nomenclature 2:3 AX indicates the waste:binder ratio and residue incorporated. >=greater than testable by flow table.

	BS EN 12457-2			EA NEN 7375	
	Cl (mg/kg)	TDS (mg/kg)	pH	Cl ε^*_{64} (mg/m^2)	UCS after (MPa)
2:3 A1	43,900	119,400	12.6	583,200	12.8
2:3 A2	30,400	88,000	12.6	369,300	12.6
2:3 A3	43,300	102,000	12.6	460,400	18.2
2:3 A4	32,500	95,100	12.6	392,100	17.1
2:3 A5	63,900	163,700	12.5	859,300	9.2

Table 3 Granular (BS EN 12457-2) and monolithic (EA NEN 7375) leach test results for the s/s products tested after 28 days curing. ε^*_{64}=Measured cumulative release over 64 days

Appendix A.

Figure A.1 shows the linear calibration curves established in order to quantify the concentration of $Ca(OH)_2$ and subsequently CaClOH, present in the as-received residues. Curves were developed by first washing the residues for twenty four hours at a liquid to solid ratio of ten in de-ionised water, a procedure which has previously been shown to remove the CaClOH [1]. The residues were then filtered and rinsed with de-ionised water to prevent any precipitation of the soluble salts, and dried in a vacuum after solvent exchange with isopropanol. The resultant residues were subjected to simultaneous thermogravimetric and differential thermal analysis with and without dilution by mixing in various weight ratios with an inert material of known thermal decomposition ($CaCO_3$). Examples of the data obtained are shown in Figure A.2. 5-7 data points were established for the calibration curves. Coefficients of determination calculated by Microsoft Excel for the linear regressions intercepting the origin were all greater than 0.96. No calibration curve could be established for residue A3 due to the initially low concentration of $Ca(OH)_2$.

Several factors, including the degree of crystallinity of the compound and crystal size, will affect the heat required for decomposition and therefore the DTA response per unit concentration [2-4]. Particle size could also affect the DTA response but pre-treatment of the residues by grinding with a pestle and mortar should have mitigated against these effects. Calibration curves were therefore established for each of the residues (A1, A2, A4 and A5) separately. Without further analysis the reason for the differences in the curve gradients cannot be identified. XRD analysis of the residues presented in Figure 1 shows clear differences in the breadth of the peaks associated with $Ca(OH)_2$ which could relate to differences in crystal size [5]. However, in order to attribute the broadening to the effects of crystal size, the residue would have to first be analysed after removal of the CaClOH phase which may produce overlapping XRD peaks resulting in apparent broadening.

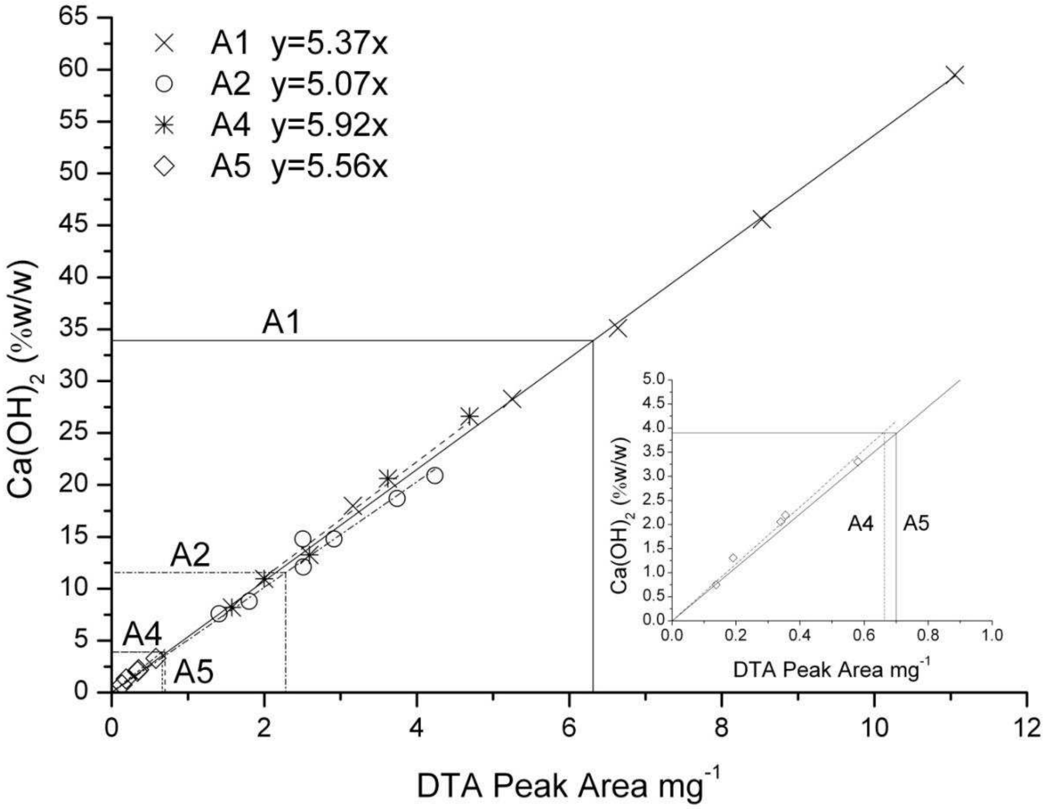

Figure A.1 Calibration curves showing DTA peak area against %w/w $Ca(OH)_2$ for residues A1, A2, A4 and A5. Drop lines indicate analysis of the as-received residues. Inset shows magnification of the lower region of the graph relevant to analysis of residues A4 and A5.

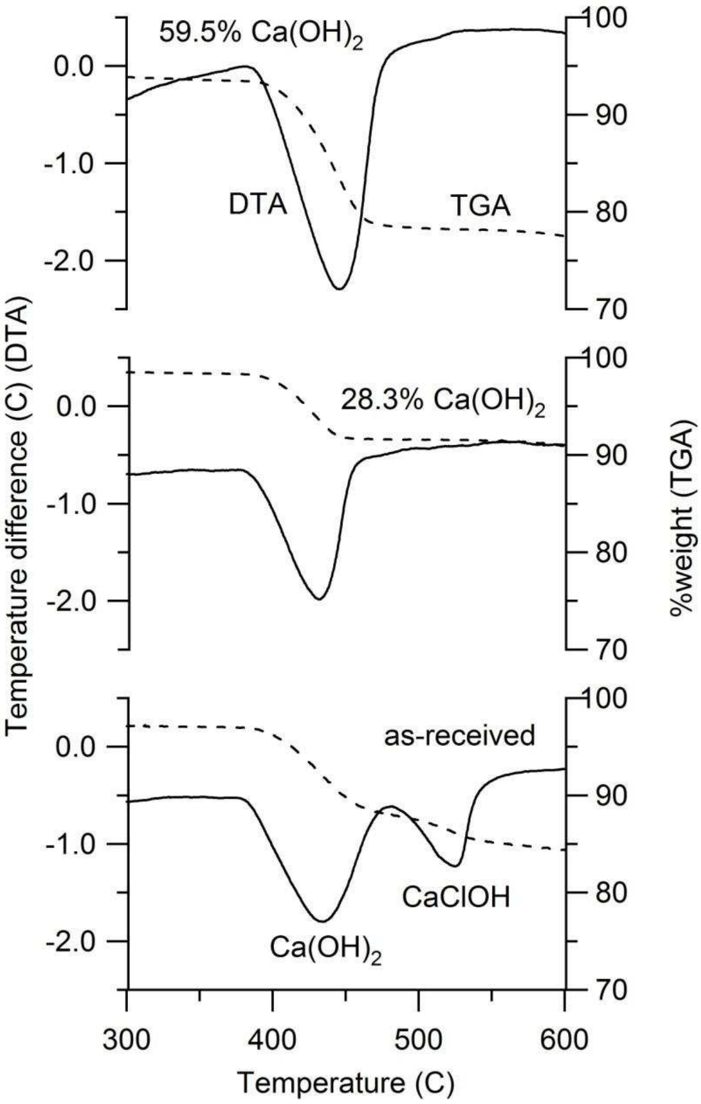

Figure A.2 Examples of STA data collected when analysing residue A1

1. Shirley R and Black L (2011) Alkali activated solidification/stabilisation of air pollution control residues and co-fired pulverised fuel ash. Journal of Hazardous Materials **194**: 232-242.
2. Odler I and Dorr H (1979) Early hydration of tricalcium silicate. I. Kinetics of the hydration process and the stoichometry of the hydration products. Cement and Concrete Research **9(2)**: 239-248.
3. Odler I, Schoppstuhl J and Dorr H (1979) Thermoanalytical studies on hydrated tricalcium silicate. Thermochimica Acta **29(2)**: 283-287.
4. van der Marel HW (1956) Quantitative differential thermal analyses of clay and other minerals. American Mineralogist 1956 **41(3-4)**: 222-244.
5. Klug HP and Alexander LE (1974) X-ray diffraction procedures for polycrystalline and amorphous materials. Wiley, New York, USA

Appendix B.

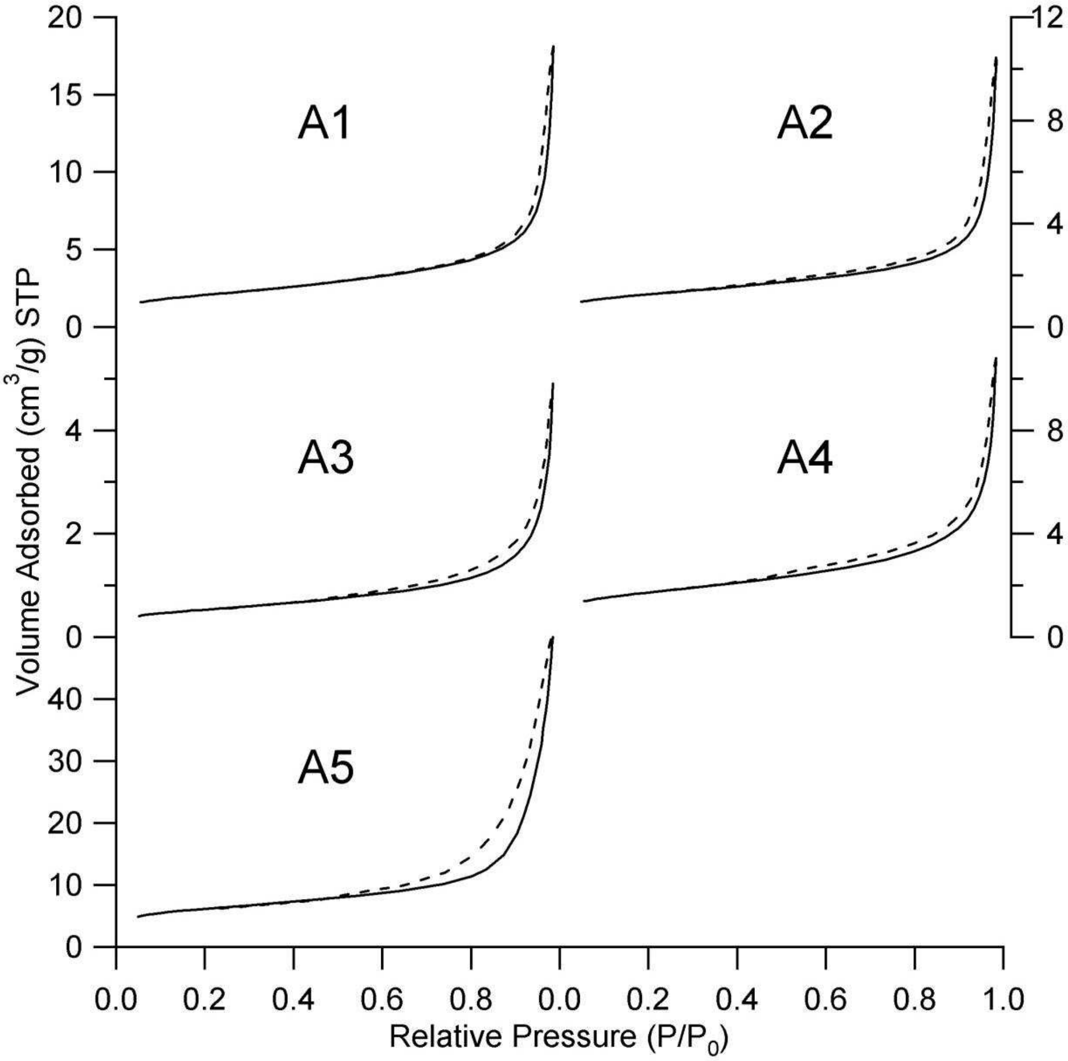

Figure B.1 N_2 sorption isotherms recorded at 77K for as-received residues. Dashed lines show desorption branches.